EPJ Web of Conferences **315**, 01029 (2024) https://doi.org/10.1051/epjconf/202431501029
LCWS2024

Search for the Exotic Decay of the Higgs Boson into a Pair of Light (Pseudo-)Scalar Higgs Boson in e^+e^- Collider

Cheng-Hsu Nee[1,*], *Abdollah* Mohammadi[1,**], and *Sridhara* Dasu[1,***]

[1]Department of Physics, University of Wisconsin-Madison, Madison, Wisconsin 53706, USA

Abstract. This study focuses on the exotic decay of the Higgs boson into a pair of light (pseudo-)scalar bosons ($h \to aa$), where the mass of a boson ranges from 10 to 60 GeV. The primary objective is to assess the sensitivity of e^+e^- collider in probing these decays, particularly in the $h \to aa \to bb\tau\tau$ channel. Advanced event generation and reconstruction techniques were employed, including tailored tau identification and a specialized b-jet identification method, to efficiently isolate signal from background events. The analysis approach allows for reconstruction of the a bosons from both the $\tau\tau$ and bb final states. The model-independent analysis resulted in a 95% confidence level upper limit on the cross-section σ ($e^+e^- \to Zh \to Zaa \to llbb\tau\tau$) and on the branching ratio BR ($h \to aa \to bb\tau\tau$). Additionally, a model-dependent analysis can be used to set a 95% confidence level upper limit on $BR(h \to aa)$ within the two-Higgs-doublet-plus-singlet (2HDM+S) models. Both analyses show sensitivity comparable to the CMS results, with improved sensitivity in the lower a boson mass region, despite utilizing only the $Z \to e^+e^-/\mu^+\mu^-$ and $h \to aa \to bb\tau\tau$ channels. In conclusion, the presented study demonstrates the strong potential of e^+e^- colliders in detecting light (pseudo-)scalar bosons, with future improvements possible through the inclusion of additional decay channels. The analysis suggests that e^+e^- collider has the potential to achieve greater sensitivity than LHC / HL-LHC.

1 Introduction

Experiments at future high-energy colliders will offer us a unique opportunity to probe uncharted territories beyond the Standard Model of particle physics. Developing colliders with higher energy and luminosity is essential to facilitate these investigations and potentially discover new physics phenomena. The Standard Model, which has been remarkably successful in explaining a wide range of particle interactions, predicts the existence of a single Higgs boson with a mass of approximately 125 GeV. However, Beyond the Standard Model (BSM) theories often introduce the existence of additional Higgs particles with varying masses and properties, providing a fertile ground for discovery. The BSM theories allow these additional Higgs bosons to either be lighter or heavier than the 125 GeV Higgs boson. Of specific interest are (pseudo-)scalar Higgs bosons with masses less than half of the 125 GeV Higgs boson, particularly those in the range of 10-60 GeV, produced in the decay channel $h \to aa$. Such

*e-mail: cnee@wisc.edu
**e-mail: mohammadi4@wisc.edu
***e-mail: dasu@hep.wisc.edu

decay represents a significant area of interest for current and future collider experiments. Furthermore, the study of the new exotic scalar production presents unique challenges. Due to their lower mass, these particles are often produced in highly boosted states, complicating their detection and analysis. As a result, specialized analysis techniques are required to effectively identify and study these boosted particles. The advancement of such techniques is crucial for the successful exploration of the full range of phenomena predicted by BSM theories, further underscoring the importance of future high-energy e^+e^- collider programs.

2 Analysis strategy

To probe the existence of a light (pseudo-)scalar Higgs boson, predicted by various BSM theories, this analysis focused on designing a comprehensive search strategy for an experiment at a future high-energy e^+e^- collider. Building upon the motivation to explore the properties of these additional lighter Higgs bosons, this analysis employs advanced event generation, selection, and reconstruction techniques to identify the unique signatures of the (pseudo-)scalar Higgs decays. The methodology presented here outlines the collider setup, signal and background processes, and the specialized analysis methods developed to enhance the sensitivity of our search.

2.1 Collider Setup and Event Generation

Considered in the presented study is an experiment at a 250 GeV center-of-mass energy e^+e^- Cool Copper Collider (C^3) [1]. This environment is set up for the production of Higgs bosons, which subsequently decay into two lighter (pseudo-)scalar bosons (denoted as a). Signal and background events were generated using MadGraph5, a Monte Carlo event generator that simulates high-energy physics processes. The generated events were hadronized using Pythia8, which models the development of parton showers and subsequent hadron formation. The hadronized events were processed with Delphes, a fast simulation framework that accounts for detector geometry and resolution effects to simulate the detector response.

2.2 Signal and Background Processes

The primary signal process under consideration is the production of a Higgs boson (h) in association with the Z boson that decays into a pair of lighter (pseudo-)scalar a bosons, where the mass of the a boson is set in the range of 20-60 GeV with a 10 GeV interval. The a bosons subsequently decay into final states consisting of b-jets ($b\bar{b}$) and tau pairs ($\tau^+\tau^-$), listed in Table.1.

Moreover, the Zh production and the ZZ production were considered as the two main background processes, listed in Table.1. For the Zh production, the Z boson decays into a pair of charged leptons ($\mu^+\mu^-/e^+e^-$), while the Higgs boson decays into any possible Standard Model final state. Moreover, for the ZZ production, one of the Z bosons decays into a pair of leptons ($\mu^+\mu^-/e^+e^-$), and the other Z boson decays into a pair of fermions ($f\bar{f}$, excluding $\mu^+\mu^-/e^+e^-$). The number of events for the signal and the background has been scaled to 2 ab^{-1} luminosity($\mathcal{L}$) for this analysis.

2.3 Reconstruction Techniques

2.3.1 Tau Reconstruction

The tau leptons were reconstructed from the energy flow (Eflow) objects (track, photons, hadrons) from the Delphes event reconstruction. The tau reconstruction algorithm begins by

Table 1: List of signal and background processes, where $ll = \mu^+\mu^-/e^+e^-$ and $f\bar{f}$ = fermions excepts $\mu^+\mu^-/e^+e^-$

Channels	σ (fb)	# of Events Generated
$e^+e^- \rightarrow Z(\rightarrow ll)\ H \rightarrow a(\rightarrow b\bar{b})\ a(\rightarrow \tau^+\tau^-)$	6.60	10000
$e^+e^- \rightarrow Z(\rightarrow ll)\ H$	6.60	1000000
$e^+e^- \rightarrow Z(\rightarrow ll)\ Z(\rightarrow f\bar{f})$	35.2	1000000

identifying a track with a transverse momentum (P_T) greater than 2 GeV. If a second track with higher P_T is found within $\Delta R = 0.5$, this new track is designated as the leading track. Any Eflow candidate within the dynamic signal cone, with a ΔR linearly varying from 0.1 at $P_T = 20$ GeV to 0.2 at $P_T = 10$ GeV, surrounding the leading track is subsequently clustered to the tau signal candidates. Additionally, the isolation of the tau candidates was quantified by summing P_T of the Eflow objects between the signal cone and the $\Delta R = 0.5$ isolation cone. Furthermore, an isolation ratio cut is applied to the tau candidates which is defined as the following:

$$\text{isolation ratio} = \frac{P_{T,\text{isolations } \tau \text{ candidate}}}{P_{T,\text{signal } \tau \text{ candidates}}} \tag{1}$$

Only τ candidates that have a maximum of 5 charged prongs and satisfy the isolation criterion cut were considered as Reconstructed taus (Reco τ).

$$\text{Matching Efficiency} = \frac{P_{T,\text{ Vis } \tau \text{ mathed to Reco } \tau}}{P_{T,\text{ Vis } \tau}} \tag{2}$$

$$\text{Purity} = \frac{P_{T,\text{ Reco } \tau \text{ mathed to Vis } \tau}}{P_{T,\text{ Reco } \tau}} \tag{3}$$

The reconstruction achieved a high matching efficiency (Eq.2) and purity (Eq.3) in the low P_T region for the hadronic τ, which is particularly significant for detecting the desired lighter a bosons (Fig.1). The matching efficiency tells us how well the reconstructed objects correspond to the generator-level particles produced in the collision event. Specifically, it is the fraction of true particles (Vis τ) that are correctly identified by the reconstruction algorithm. Purity is a measure of how many of the reconstructed particles are correctly matched to the true particles (Vis τ). It reflects the proportion of reconstructed objects that are the particles of interest, rather than background or misidentified particles, for example, the b-jets. A one-to-one matching of hadronic visible τ (Vis τ) in Gen-level to hadronic Reco τ was achieved within a $\Delta R = 0.5$, where the Vis τ was matched to the closest Reco τ. This demonstrates the effectiveness of our tau identification approach. For subsequent analysis, an isolation criterion cut of 0.3 was selected as it optimally balances the need to preserve a significant portion of the signal while effectively suppressing background events.

The τ reconstruction process mentioned above is considered a track-based reconstruction process in which the Reco τ aligns in the same direction as the leading track. On the contrary, a photon-based reconstruction process has been considered but overall, it didn't improve the result significantly.

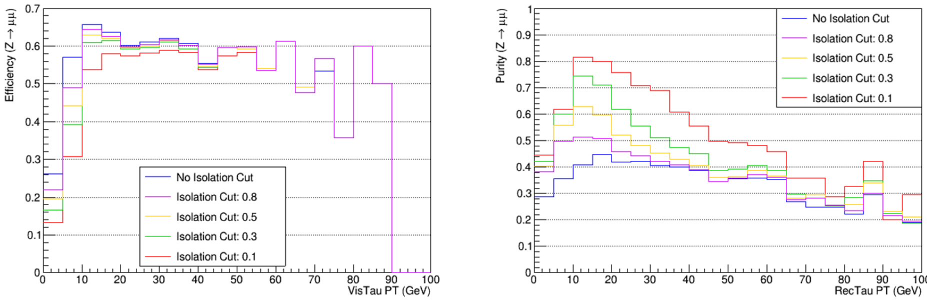

Figure 1: Both plots are derived from the signal process with a boson mass of 30 GeV. (Left) The efficiency of matching hadronic Vis τ transverse momentum (p_T) with $Z \to \mu^+\mu^-$. Different isolation ratio cuts (0.1, 0.3, 0.5, 0.8) are compared against no isolation cut. (Right) Purity of matching hadronic Reco τ transverse momentum (p_T) under the same conditions. The plots illustrate the impact of various isolation ratio cuts on both the efficiency and purity of tau reconstruction across different p_T regions.

2.3.2 Rest of Events (ROE) Reconstruction

The reconstructed Rest of Events (RecROE) approach was implemented using EFlow objects as follows:

$$\text{RecROE} = \sum_i^{\text{excl } l \ \& \ \tau} \text{tracks}_i + \sum_i^{\text{excl } l \ \& \ \tau} \text{Photons}_i + \sum_i^{\text{excl } l \ \& \ \tau} \text{NHadrons}_i \tag{4}$$

This reconstruction approach accounts for all hadronic activity, excluding contributions from the selected leptons ($\mu^+\mu^-$ / e^+e^-) resulting from the Z boson decay and taus ($\tau^+\tau^-$) from the other a boson decay. The exclusion criterion removes all the selected leptons and taus within $\Delta R = 0.2$ cone from the RecROE. This technique avoided the limitations of the traditional jet reconstruction algorithm from Delphes and resulted in a more efficient signal selection (Shown in Fig.2).

In Figure2, the RecROE reconstruction is shown for $Z \to \mu^+\mu^-$ (blue histogram) and $Z \to e^+e^-$ (red histogram), while the Delphes reconstruction is shown for $Z \to \mu^+\mu^-$ (green histogram) and $Z \to e^+e^-$ (purple histogram). The RecROE approach demonstrates a significant improvement in the reconstruction of b-jet pairs, where the efficiency of selecting a pair of b-jets using the Delphes jet reconstruction algorithm is only 15%, see Fig.2.

2.4 Event Selection

To isolate signal events from the backgrounds, a series of selection criteria were applied:

- Lepton Pair Selection: Events were required to contain a pair of oppositely charged leptons, $\mu^+\mu^-$ or e^+e^- , consistent with the Z boson decay. The leptons were reconstructed using the Delphes muons or electrons reconstruction algorithm.
- Tau Pair Selection: Events were also required to contain a pair of oppositely charged taus. Tau reconstruction was performed using energy flow (EFlow) data from Delphes, which includes information from tracks, photons, and neutral hadrons. This is discussed previously in section 2.3.1

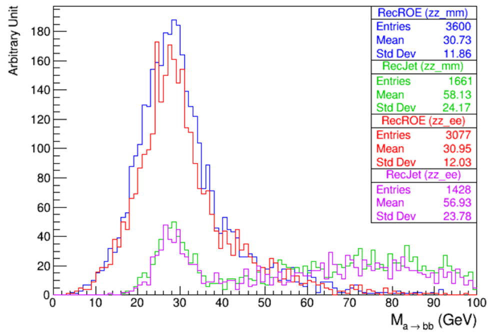

Figure 2: Comparison of the invariant mass distributions $M_{inv,\, b\bar{b}}$ for b-jets reconstructed using the RecROE and Delphes methods.

- Rest of Events (ROE) Selection: To represent b-jets, instead of direct selection, the Rest of Events (ROE) method was employed, which reconstructs the b-jets not associated with the leptons ($\mu^+\mu^-/e^+e^-$) or taus ($\tau^+\tau^-$). This approach eliminates the need for the jet reconstruction algorithm from Delphes, thereby improving signal efficiency, as discussed in detail in section 2.3.2.

3 Results

This analysis relies on the precise reconstruction of events involving the production of the light (pseudo)-scalar a boson, enabling differentiation from various background processes. This involves applying a series of event selection criteria designed to maximize the efficiency of identifying the unique decay products of the Higgs boson while minimizing the background events. By examining the performance of this selection, the accuracy and effectiveness of our techniques can be assessed, laying the foundation for further analysis of the Higgs boson decay products.

3.1 Z Bosons Reconstruction

The reconstruction of leptonic Z boson decays is a key aspect of our analysis, providing a distinct signature that helps differentiate events where the Z boson is fully reconstructed from those where it is not. This analysis has focused on events containing a pair of oppositely charged $\mu^+\mu^-$ or e^+e^- consistent with a Z boson decay. This initial selection is crucial to isolate the events of interest while minimizing contributions from background processes.

The Z boson mass was reconstructed by combining the four-momenta of the selected lepton pair. This approach resulted in a reconstruction efficiency of approximately 73% (for $Z \to \mu^+\mu^-$) or 62% (for $Z \to e^+e^-$), with a clear mass peak observed around 91 GeV (Shown in Fig. 3). This peak matches the known mass of the Z boson in the Standard Model, confirming the effectiveness of our selection criteria. The successful reconstruction of the Z boson mass establishes a solid foundation for the subsequent steps of our analysis, focusing on detecting the a bosons.

3.2 a Bosons Reconstruction

The subsequent phase of the analysis was focused on reconstructing the a boson using the τ-pair objects, as detailed in Section 2.3.1, in conjunction with missing transverse energy. For

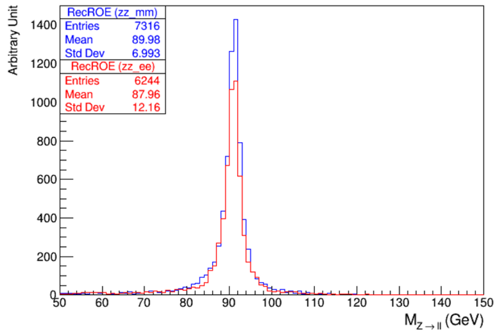

Figure 3: Comparison of the invariant mass distributions $M_{inv,\,Z}$ for $Z \to \mu^+\mu^-$ (blue histogram) and $Z \to e^+e^-$ (red histogram) events.

the study of a boson reconstruction, the invariant mass of the a boson was set to 30 GeV. At the generator (Gen) level, the invariant mass distribution of the a boson, reconstructed from visible tau (Vis τ) pairs, peaked at approximately 20 GeV, which is lower than the assumed mass of the a boson. This discrepancy is due to the undetected momenta of neutrinos produced in tau decays. By incorporating GenMET, defined as the negative sum of the transverse momentum and energy of the generator-level particles, the peak shifted to around 30 GeV, aligning with the hypothesized a boson mass. At the reconstructed (Reco) level, a similar procedure was applied. Initially, the mass peaked at approximately 20 GeV; however, after incorporating MET, defined as the negative sum of the transverse momentum and energy of the reconstructed-level particles, the distribution was adjusted accordingly. Once MET was accounted for, the mass peak shifted to approximately 30 GeV, consistent with the expected a boson mass. This observation holds for both Z boson decay channels considered, $Z \to \mu^+\mu^-$ and $Z \to e^+e^-$. The selection efficiency at the Reco level was found to be 36% for the $Z \to \mu^+\mu^-$ channel and 30% for the $Z \to e^+e^-$ process (Shown in Fig.4).

For both plots in Figure 4, the blue histogram represents the mass distribution of the a boson reconstructed from Vis τ pairs. The red histogram depicts the corrected mass distribution after incorporating GenMET. The green histogram corresponds to the Reco τ mass distribution at the Reco level, and the purple histogram illustrates the adjusted mass distribution after accounting for MET at the Reco level. These distributions demonstrate the importance of including MET and GenMET corrections for improving the reconstructed mass resolution, particularly at the Reco level.

Instead of using the Delphes jet reconstruction algorithm, the Rest of the Events method was employed to reconstruct the a bosons, which is in detail explained in section 2.3.2. This approach achieved a peak position around 30 GeV for both Gen-level (GenROE) and Reco-level (RecROE), aligning with the set mass for a boson. The selection efficiency at the Reco level was found to be 36% for the $Z \to \mu^+\mu^-$ process and 30% for the $Z \to e^+e^-$ process (Shown in Fig.5)

For both plots in Figure 5, the blue histogram represents the mass distribution of the a boson reconstructed from Vis τ pairs. The red histogram depicts the corrected mass distribution after incorporating GenMET. The green histogram corresponds to the Reco τ mass distribution at the Reco level, and the purple histogram illustrates the adjusted mass distribution after accounting for MET at the Reco level. These results highlight that incorporating MET corrections significantly improves the reconstructed mass resolution, particularly for distributions at the Reco level, and aligns them more closely with the expected values.

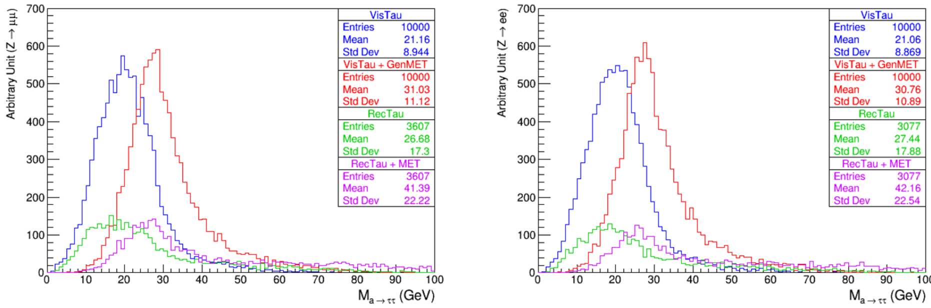

Figure 4: A comparison of the reconstructed a boson mass distributions from τ-pair at both the generator (Gen) and reconstructed (Reco) levels is presented. The left panel illustrates the comparison for the $Z \to \mu^+\mu^-$ process, while the right panel shows the comparison for the $Z \to e^+e^-$ process.

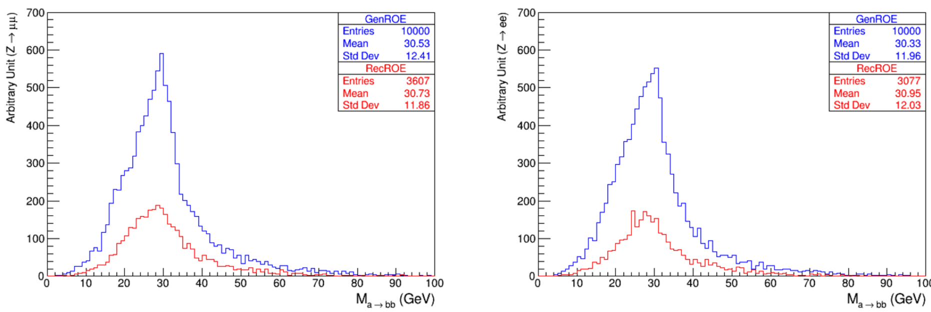

Figure 5: A comparison of the reconstructed a boson mass distributions from ROE at both the generator (Gen) and reconstructed (Reco) levels is presented. The left panel illustrates the comparison for the $Z \to \mu^+\mu^-$ process, while the right panel shows the comparison for the $Z \to e^+e^-$ process.

3.3 Higgs Bosons Mass Reconstruction

In the analysis of the Higgs boson mass, at the Gen level, the invariant mass of the visible Higgs boson, constructed from the Vis τ and GenROE components (illustrated in red in Fig.6a), and the Reco Higgs boson, formed from the Reco τ and RecROE components (illustrated in green in Fig.6a), both exhibit mass peaks around 100 GeV. However, these peaks are relatively broad, due to the effect of four-momenta carried away by neutrinos from τ lepton decays, which impacts the accuracy of the mass reconstruction.

By including the GenMET in the visible Higgs boson reconstruction (illustrated in red in Fig.6b) and the MET in the Reco Higgs boson reconstruction (illustrated in green in Fig.6b), the mass peaks become more pronounced and shift closer to the generator-level Higgs boson mass (illustrated in blue in Fig.6b), which exhibits a sharp peak at 125 GeV. This suggests that the inclusion of GenMET and MET substantially improves the accuracy of the Higgs boson mass reconstruction.

Although the incorporation of MET improves the precision of the Higgs boson mass reconstruction, there remain opportunities for further Higgs boson mass resolution improvement. Given the center-of-mass energy of the collision is 250 GeV, and the high reconstruction efficiency on the Z boson, this analysis employs computing the recoil Higgs boson Mass

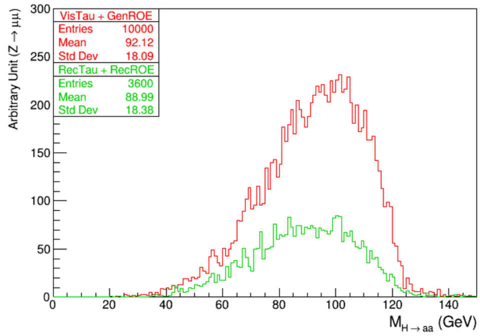

(a) Reconstructing the Higgs boson from τ-pair and ROE components.

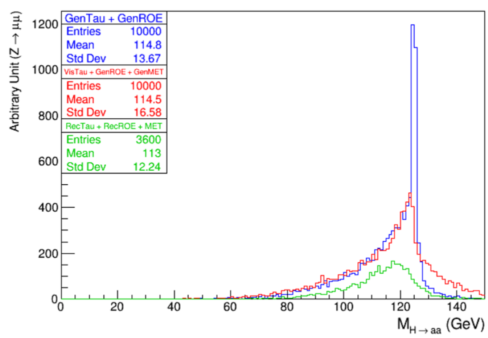

(b) Reconstructing the Higgs boson from τ-pair, ROE, GenMET, and MET.

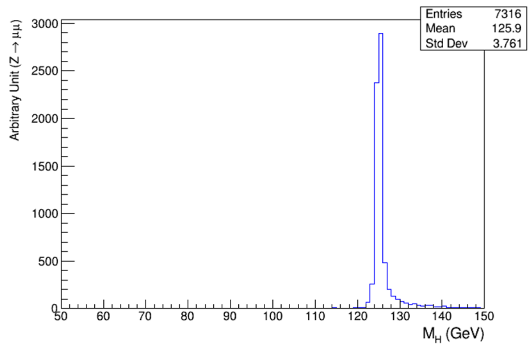

(c) Direct reconstruction of the Higgs boson from Eq.5 using beam constraints and the Z boson.

Figure 6: This figure illustrates different methods for reconstructing the Higgs boson mass.

against the Z boson (M_{Rec}) directly by using the following formula [2]:

$$M_{Rec}^2 = s + M_{Rec,Z}^2 - 2E_{Rec,Z}\sqrt{s} \tag{5}$$

where $M_{Rec,Z}$ is the the mass of the Reco Z boson, $E_{Rec,Z}$ is the the energy of the Reco Z boson, and s is the center-of-mass energy which is 250 Gev for this analysis.

This approach yields a sharp mass peak at 125 GeV for M_{Rec}, shown in Fig.6c, indicating that the reconstruction accuracy of the Higgs boson mass is significantly enhanced when using the beam constraint method compared to the method based on τ-pair and ROE components.

3.4 Final Observables and Signal Extraction

To isolate the signal more effectively, a series of kinematic cuts were applied to the mass ranges for the Higgs boson and for the two a boson candidates. For the Higgs boson, the selected mass range was between 115-135 GeV, and for the a boson, selected was the range of 0-70 GeV for both τ-pair and ROE components. These cuts substantially reduce background events, particularly from the ZZ process, thereby allowing a clearer focus on potential signal events. Figure 7 illustrates the mass distributions for the selected a boson and Higgs boson, the a boson mass is shown for signal events at 20 GeV (blue), 30 GeV (red), 40 GeV (green), 50 GeV (yellow), and 60 GeV (magenta), as well as for the ZZ background (cyan) and Zh background (grey) that passed the selection criteria.

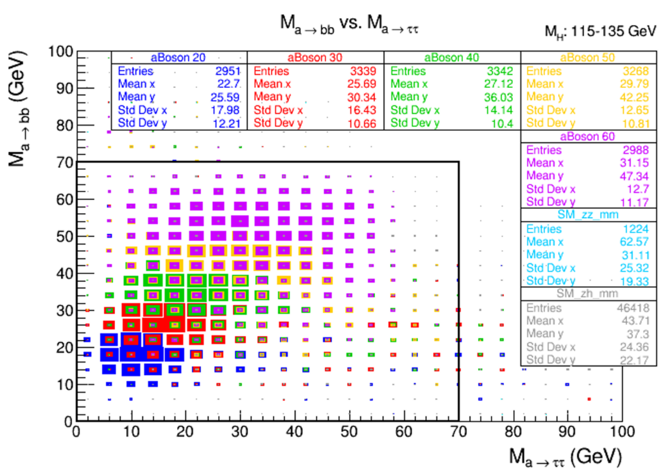

Figure 7: A 2D scatter plot comparing the M_{inv} (only 20-60 GeV) of the a boson reconstructed from RecROE (y-axis); and the M_{inv} of the a boson reconstructed from diRecτ for the $Z \to \mu^+\mu^-$ process. The solid black line represents the cuts on the a boson.

These Two-dimensional scatter plots (Figure 7) were then converted into one-dimensional histograms to better visualize the mass limits for both signal and background events shown in Fig.8. The final observables derived from these plots were use to extracting upper limits on the Higgs boson cross-section and branching ratios for $h \to aa$.

4 Model-Independent and Model-Dependent Limits

4.1 Model-Independent Limit

A maximum likelihood fit was employed to extract the expected limit. Minimal systematic uncertainties were assumed, with 0.2% assigned to the cross-sections of both signal and background events. Additionally, uncertainties associated with lepton reconstruction, identification, and isolation, which impact the normalization of the process, were set to 1% for

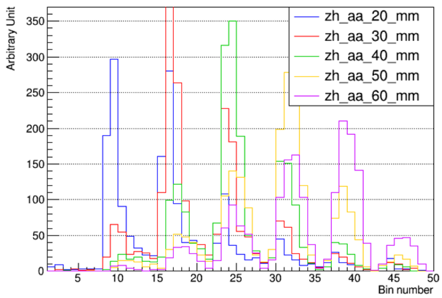

(a) $Z(\rightarrow \mu\mu)\ h(\rightarrow aa)$ unrolled histogram

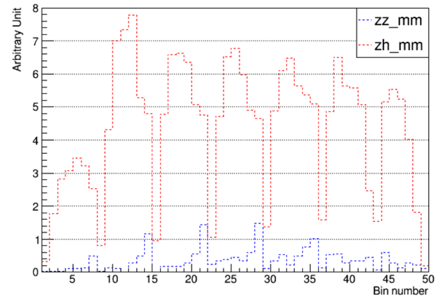

(b) $Z(\rightarrow \mu\mu)\ Z(\rightarrow ff)$ and $Z(\rightarrow \mu\mu)\ h(\rightarrow$ anything) unrolled histogram

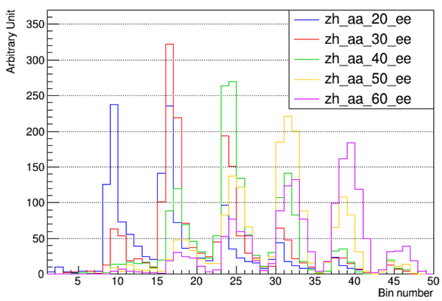

(c) $Z(\rightarrow ee)\ h(\rightarrow aa)$ unrolled histogram

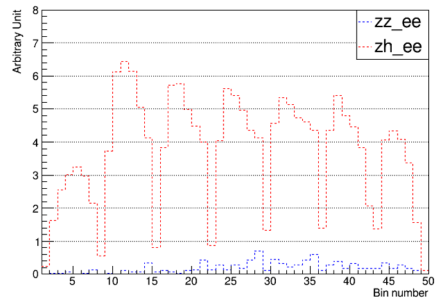

(d) $Z(\rightarrow ee)\ Z(\rightarrow ff)$ and $Z(\rightarrow ee)\ h(\rightarrow$ anything) unrolled histogram

Figure 8: Comparison of different unrolled 1D observables histograms in the context of BSM and SM Higgs decays. Each subplot represents a different analysis scenario.

muons and electrons and 2% for taus. The limits were produced at 2 ab^{-1} luminosity and center-of-mass energy of 250 GeV in the C^3 collider simulation.

As illustrated in Fig.9, the left plot depicts the corresponding 95% confidence level (CL) limit on the production cross section $\sigma(Zh \rightarrow Zaa \rightarrow llbb\tau\tau)$ for the a boson mass range from 10-60 GeV demonstrating the expected limit with ($\pm1\sigma$) and ($\pm2\sigma$) variations. The right plot in Fig.9, on the other hand, shows the 95% CL branching ratio (BR) limit on $h \rightarrow aa \rightarrow bb\tau\tau$ as a function of the a boson mass (m_a), ranging from 10–60 GeV. This limit is similarly accompanied by ($\pm1\sigma$) and ($\pm2\sigma$) bands to reflect variations. This BR limit on $h \rightarrow aa \rightarrow bb\tau\tau$ is derived using the following equation:

$$BR\ (h \rightarrow aa \rightarrow bb\tau\tau) = \frac{\sigma_{Zh\rightarrow Zaa\rightarrow llbb\tau\tau}}{\sigma_{\text{SM},\,Zh} \times BR_{Z\rightarrow ll}} \tag{6}$$

where $\sigma_{Zh\rightarrow Zaa\rightarrow llbb\tau\tau}$ is obtained from the left plot in Fig.9, $\sigma_{\text{SM},\,Zh} = 6.603$ fb, and $BR_{Z\rightarrow ll} = 0.067$ for $ll = \mu\mu/ee$.

This study demonstrates higher sensitivity in measuring $\sigma(Zh \rightarrow Zaa \rightarrow llbb\tau\tau)$ and $BR(h \rightarrow aa \rightarrow bb\tau\tau)$ for the C^3 collider at 2 ab^{-1} luminosity, particularly in the lower mass region, compared to the CMS experiment on analysis of the data corresponding to the integrated luminosity of 138 fb^{-1} at 13 TeV [3]. For instance, as shown in Fig.9, at $m_a = 10$

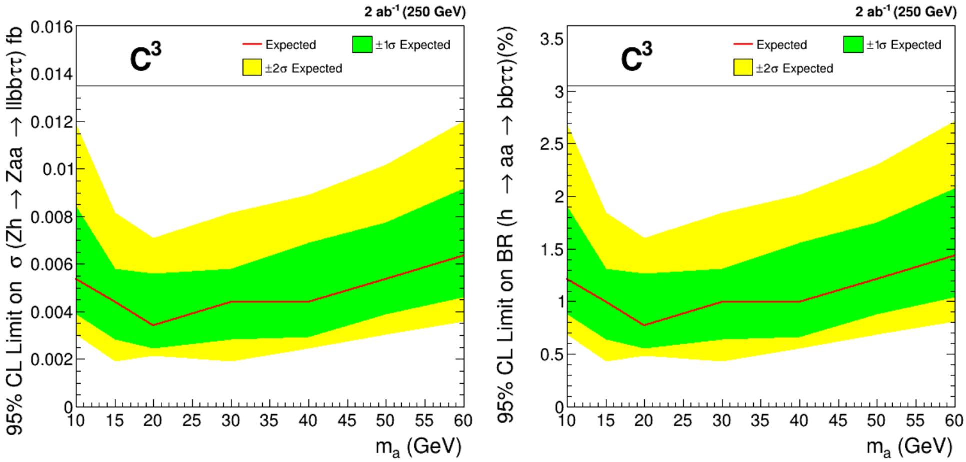

Figure 9: (Left) 95% CL upper limit on σ $(Zh \to Zaa \to llbb\tau\tau)$ for C^3 in 2 ab^{-1} luminosity at 250 GeV. (Right) 95% CL upper limit on BR $(h \to aa \to bb\tau\tau)$ limit for C^3 in 2 ab^{-1} luminosity at 250 GeV

GeV, the branching ratio limit $h \to aa \to bb\tau\tau$ from our analysis is 1.2%, significantly better than the CMS limit of 4.3%. Similarly, 1% limit was achieved in this analysis, while CMS reports approximately 3.7%. These results highlight the enhanced sensitivity of the e^+e^- collider in probing low-mass a-bosons.

Furthermore, even at m_a = 40 GeV, where the differences are less pronounced, our analysis reaches a branching ratio BR_{C3} $(H \to a_1 a_1 \to \tau\tau bb)$ of approximately 1%, compared to BR_{CMS} $(H \to a_1 a_1 \to \tau\tau bb)$ around 1.7%. This consistent improvement in sensitivity emphasizes the potential of the e^+e^- collider for exploring $h \to aa$ decay.

It is also important to note that this study currently utilizes only the $Z \to e^+e^-$ and $Z \to \mu^+\mu^-$ channels. By incorporating additional decay channels, such as neutrino $(Z \to \nu\bar{\nu})$ and hadronic $(Z \to q\bar{q})$ modes, the sensitivity of our results can be further enhanced, offering a promising path for future studies.

4.2 Model-Dependent Limit Extraction Using 2HDM

The model-dependent limit analysis employs the predictions of the Two-Higgs-Doublet plus a Singlet model (2HDM+S) [4] to extract the limit on $h \to aa$. This limit is derived using the following equation:

$$BR\,(h \to aa) = \frac{\sigma_{Zh \to Zaa \to llbb\tau\tau}}{\sigma_{SM,\,Zh} \times BR_{Z \to ll} \times BR_{a \to bb} \times BR_{a \to \tau\tau}} \tag{7}$$

where $\sigma_{Zh \to Zaa \to llbb\tau\tau}$ is the cross section limit from the model-independent analysis, $\sigma_{\mathrm{SM},\,Zh}$ = 6.603 fb from genereated Madgragh background events, and $BR_{Z \to ll}$ = 0.067 for $ll = \mu\mu/ee$ [5].

The branching ratios $BR_{a \to bb}$ and $BR_{a \to \tau\tau}$ are obtained from [4]. In this study, the 2HDM+S Type II with $\tan\beta$ = 5 and 2HDM+S Type I is used as a representative example. The values for $BR_{a \to bb}$ and $BR_{a \to \tau\tau}$ for the 2HDM+S Type II with $\tan\beta$ = 5 model are shown in Table.2 and 2HDM+S Type1 model are shown in Table.3 .

The plots in Fig. 10 present the branching ratios for the pseudoscalar $h \to aa$ relative to Standard Model (SM) expectations, providing insight into the behavior of the pseudoscalar a

boson over a mass range of 10–60 GeV. The left plot in Fig.10 illustrates the 2HDM+S Type II model with $\tan\beta = 5.0 \tan\beta = 5.0$. The observed limit falls approximately within the range of 18% to 22% for m_a values between 10 and 40 GeV. The right plot in Fig. 10 represents the 2HDM+S Type1 model, the observed limit is approximately 27% at $m_a \approx 15$ GeV and 26% at $m_a \approx 40$ GeV.

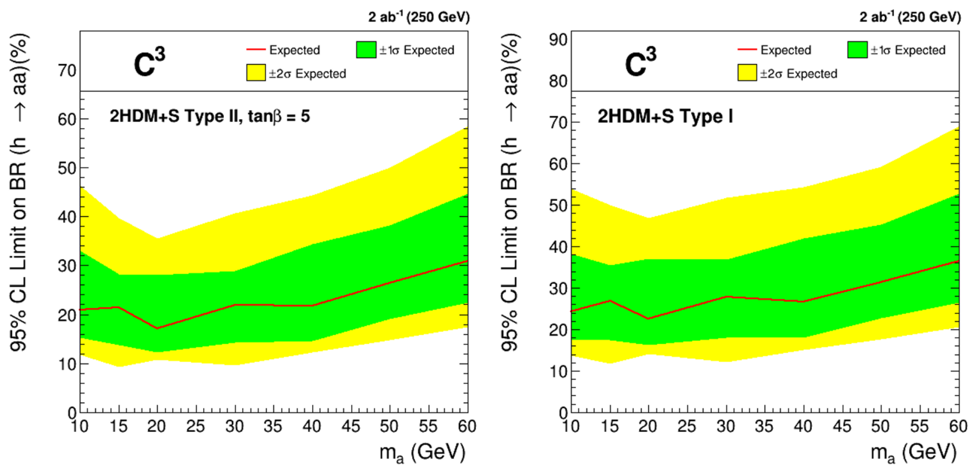

Figure 10: Comparison of the expected 95% CL limits on the branching ratio (BR) for $h \to aa$ in different 2HDM+S models Type2 with $\tan\beta = 5$ and Type1 across various a boson masses.

a Boson Mass (GeV)	$BR_{a\to bb}$	$BR_{a\to\tau\tau}$
10	0.92	0.063
15	0.93	0.05
20	0.93	0.0485
30	0.93	0.0488
40	0.93	0.049
50	0.93	0.0495
60	0.93	0.05

Table 2: Branching ratios $BR(a \to \text{SM})$ for the 2HDM+S Type2 model with $\tan\beta = 5$. [4]

a Boson Mass (GeV)	$BR_{a\to bb}$	$BR_{a\to\tau\tau}$
10	0.78	0.064
15	0.82	0.045
20	0.9	0.038
30	0.89	0.04
40	0.885	0.042
50	0.88	0.044
60	0.875	0.045

Table 3: Branching ratios $BR(a \to \text{SM})$ for the 2HDM+S Type1 model. [4]

The $BR(h \to aa)$ limit extracted from the C^3 analysis shows higher sensitivity to the CMS results[3], it is important to recognize that this comparison is made under different model assumptions. Specifically, CMS employs $\tan\beta = 2.0$, while the C^3 analysis uses $\tan\beta = 5.0$; however, this difference does not significantly impact the final results.

When the LHC is upgraded to the HL-LHC and reaches a luminosity of 1 ab^{-1}, CMS might not be able to directly inherit the results from Run II. Since the C^3 analysis focuses on a light or soft (pseudo-)scalar a boson, the trigger efficiency at HL-LHC could be degraded due to a significant increase in background events and trigger pile-ups. Consequently, the expected sensitivity improvements at HL-LHC might not fully materialize, especially in the lower mass region of the a boson. In contrast, the C^3 analysis has the potential to improve its sensitivity by incorporating additional Z boson decay channels, such as the neutrino ($Z \to \nu\bar{\nu}$) and hadronic decays ($Z \to q\bar{q}$), which could enable it to continue outperforming CMS at the HL-LHC, building on its existing advantage over CMS at the LHC.

5 Conclusion

This study has explored the potential for identifying exotic Higgs decays into pairs of light scalar bosons ($h \to aa$) at a future high-energy e^+e^- collider, targeting a bosons with masses between 10 and 60 GeV. The analysis primarily focused on the $Zh \to Zaa \to llbb\tau\tau$ decay channel, where a bosons were successfully reconstructed from both $\tau\tau$ and bb final states. This was achieved through sophisticated event simulation, precise tau identification, and the Rest of the Events techniques. The model-independent investigation established stringent 95% confidence level upper limits on the cross-section $\sigma(Zh \to Zaa \to llbb\tau\tau)$ and the branching ratio $BR(h \to aa \to bb\tau\tau)$. Complementary model-dependent analyses within the context of two-Higgs-doublet-plus-singlet (2HDM+S) frameworks further provide the limit on $BR(h \to aa)$. Limits in this analysis demonstrated sensitivity levels higher than those achieved by the CMS experiment, with particularly enhanced performance in the lower a boson mass range. Although only the $Z \to e^+e^-/\mu^+\mu^-$ channels were utilized, the findings suggest that the e^+e^- collider holds significant potential for surpassing the LHC and even HL-LHC in the detection of light (pseudo-)scalar bosons. Expanding the analysis to include additional Z boson decay modes, such as neutrino and hadronic decays, could further enhance the collider's sensitivity, paving the way for future discoveries.

References

[1] S. Dasu, E.A. Nanni, M.E. Peskin, C. Vernieri, T. Barklow, R. Bartoldus, P.C. Bhat, K. Black, J. Brau, M. Breidenbach et al., Strategy for understanding the higgs physics: The cool copper collider (2022), 2203.07646, https://arxiv.org/abs/2203.07646

[2] J. Yan, S. Watanuki, K. Fujii, A. Ishikawa, D. Jeans, J. Strube, J. Tian, H. Yamamoto, Measurement of the higgs boson mass and $e^+e^- \rightarrow zh$ cross section using $z \rightarrow \mu^+\mu^-$ and $z \rightarrow e^+e^-$ at the ilc, Phys. Rev. D **94**, 113002 (2016). 10.1103/PhysRevD.94.113002

[3] A. Hayrapetyan, A. Tumasyan, W. Adam, J.W. Andrejkovic, T. Bergauer, S. Chatterjee, K. Damanakis, M. Dragicevic, A.E. Del Valle, P.S. Hussain et al., Search for exotic decays of the higgs boson to a pair of pseudoscalars in the $\mu\mu$bb and $\tau\tau$bb final states, The European Physical Journal C **84** (2024). 10.1140/epjc/s10052-024-12727-4

[4] D. Curtin, R. Essig, S. Gori, P. Jaiswal, A. Katz, T. Liu, Z. Liu, D. McKeen, J. Shelton, M. Strassler et al., Exotic decays of the 125 gev higgs boson, Physical Review D **90** (2014). 10.1103/physrevd.90.075004

[5] S. Navas et al. (Particle Data Group), Review of particle physics, Phys. Rev. D **110**, 030001 (2024). 10.1103/PhysRevD.110.030001